

## Impact of Clustering on the ${}^8\text{Li}$ $\beta$ Decay and Recoil Form Factors

G. H. Sargsyan<sup>1</sup>, K. D. Launey<sup>1</sup>, M. T. Burkey<sup>2,3,4</sup>, A. T. Gallant<sup>4</sup>, N. D. Scielzo<sup>4</sup>, G. Savard<sup>3</sup>, A. Mercenne<sup>1,5</sup>, T. Dytrych<sup>1,6</sup>, D. Langr<sup>7</sup>, L. Varriano<sup>2,3</sup>, B. Longfellow<sup>4</sup>, T. Y. Hirsh<sup>8</sup>, and J. P. Draayer<sup>1</sup>

<sup>1</sup>*Department of Physics and Astronomy, Louisiana State University, Baton Rouge, Louisiana 70803, USA*

<sup>2</sup>*Department of Physics, University of Chicago, Chicago, Illinois 60637, USA*

<sup>3</sup>*Physics Division, Argonne National Laboratory, Argonne, Illinois 60439, USA*

<sup>4</sup>*Lawrence Livermore National Laboratory, Livermore, California 94550, USA*

<sup>5</sup>*Center for Theoretical Physics, Sloane Physics Laboratory, Yale University, New Haven, Connecticut 06520, USA*

<sup>6</sup>*Nuclear Physics Institute of the Czech Academy of Sciences, 250 68 Řež, Czech Republic*

<sup>7</sup>*Department of Computer Systems, Faculty of Information Technology, Czech Technical University in Prague, Prague 16000, Czech Republic*

<sup>8</sup>*Soreq Nuclear Research Center, Yavne 81800, Israel*



(Received 15 August 2021; accepted 4 April 2022; published 19 May 2022)

We place unprecedented constraints on recoil corrections in the  $\beta$  decay of  ${}^8\text{Li}$ , by identifying a strong correlation between them and the  ${}^8\text{Li}$  ground state quadrupole moment in large-scale *ab initio* calculations. The results are essential for improving the sensitivity of high-precision experiments that probe the weak interaction theory and test physics beyond the standard model. In addition, our calculations predict a  $2^+$  state of the  $\alpha + \alpha$  system that is energetically accessible to  $\beta$  decay but has not been observed in the experimental  ${}^8\text{Be}$  energy spectrum, and has an important effect on the recoil corrections and  $\beta$  decay for the  $A = 8$  systems. This state and an associated  $0^+$  state are notoriously difficult to model due to their cluster structure and collective correlations, but become feasible for calculations in the *ab initio* symmetry-adapted no-core shell-model framework.

DOI: [10.1103/PhysRevLett.128.202503](https://doi.org/10.1103/PhysRevLett.128.202503)

**Introduction.**—The left-handed vector minus axial-vector ( $V - A$ ) structure of the weak interaction was postulated in the late 1950s and early 1960s [1,2] guided in large part by a series of  $\beta$ -decay experiments [3–5], and later was incorporated in the standard model of particle physics. However, in its most general form, the weak interaction can also have scalar, tensor, and pseudoscalar terms as well as right-handed currents.

Today,  $\beta$ -decay experiments continue to pursue increasingly sensitive searches for additional contributions to the weak interaction. Various experiments [5–8] have constrained the tensor part of the interaction, although the limits are less stringent compared with the other nonstandard-model terms [9,10]. While these experiments have achieved remarkable precision, further improvements require confronting the systematic uncertainties that stem from higher-order corrections (referred to as recoil-order terms) in nuclear  $\beta$  decay. These terms are inherently small compared with the allowed  $\beta$  decay terms; however, current experiments have reached a precision where even subtle distortions matter. Measurements of recoil-order terms are also interesting in their own right as they can test additional symmetries of the standard model, such as the existence of second-class currents [11–13] and the accuracy of the conserved vector current (CVC) hypothesis [12,14–16].

The  $\beta$  decay of  ${}^8\text{Li}$  to  ${}^8\text{Be}$ , which subsequently breaks up into two  $\alpha$  particles, has long been recognized as an

excellent testing ground to search for new physics [11,14,17] due to the high decay energy and the ease of detecting the  $\beta$  and two  $\alpha$  particles. Recently, by taking advantage of ion-trapping techniques, high-precision measurements of  $\beta - \bar{\nu} - \alpha$  correlations [7,8,18] have been performed that set the most stringent limit on a tensor contribution to date [19]. However, in this type of experiment, one of the largest uncertainties comes from the several different recoil-order corrections that contribute to the decay. A number of other experiments have taken advantage of the presence of certain recoil-order terms in the  $\beta$  decay of  ${}^8\text{Li}$  (Fig. 1) to perform CVC tests by studying  $\beta - \alpha$  angular correlations [15,20] and  $\beta$ -spin alignment correlations [13,16]. In addition, these terms have been deduced from  $\gamma$  decays of the doublet  $2^+$  states near 17 MeV in the  ${}^8\text{Be}$  spectrum, which contain the isobaric analog of the  ${}^8\text{Li}$  ground state (g.s.) [12]. Due to their small size, and the fact that there are several terms that contribute to decay observables, most of the experimentally extracted recoil-order terms have large uncertainties.

In this Letter, we report the first *ab initio* calculations of recoil-order terms in the  $\beta$  decay of  ${}^8\text{Li}$ . These calculations achieve highly reduced uncertainties compared with the experimentally extracted values of Ref. [16]. They help decrease the systematic uncertainties on the tensor-current estimates in the weak interaction reported in Ref. [19], and

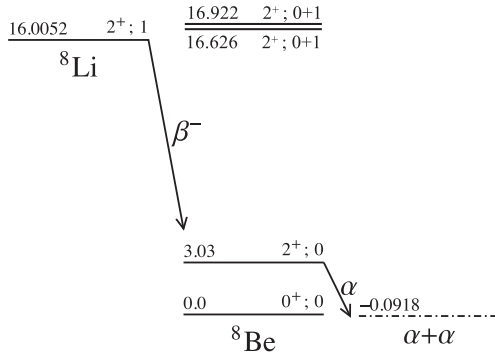


FIG. 1. Decay scheme for  $\beta$  decay of  ${}^8\text{Li}$  g.s. to the broad low-lying  $2^+$  state in  ${}^8\text{Be}$ . Energies, in MeV, are relative to  ${}^8\text{Be}$  g.s. A small  $\beta$ -decay branching is observed to the doublet  $2^+$  states due to their resonant nature.

are of interest to experimental tests of the CVC hypothesis [12]. We also provide evidence that the  $\beta$ -transition strength of the  ${}^8\text{Li}$  decay is affected by a disputed low-lying  $2^+$  state (sometimes referred to as an “intruder” state) below 16 MeV in the  ${}^8\text{Be}$  spectrum. Our calculations in unprecedentedly large model spaces support the existence of low-lying states with a large overlap with the  $\alpha + \alpha$  and  $d$  waves. Indeed, a very broad  $2^+$  state along with a lower  $0^+$  were initially proposed by Barker from the  $R$ -matrix analysis of  $\alpha + \alpha$  scattering and the  $\beta$  decays of  ${}^8\text{Li}$  and  ${}^8\text{B}$  [21–23]. Even though such states have not been directly observed experimentally, some earlier theoretical studies have predicted them in the low-lying spectrum of  ${}^8\text{Be}$  [24–26]. Furthermore, there has been a recent experimental indication in favor of intruder states below 16 MeV [27].

*SA-NCSM framework.*—For this Letter, we employ the *ab initio* symmetry-adapted no-core shell model (SA-NCSM) [28–30]. The use of chiral effective-field-theory interactions [31–34] enables nuclear calculations informed by elementary particle physics, while the symmetry-adapted (SA) basis allows us to achieve ultralarge model spaces imperative for the description of challenging features in the  ${}^8\text{Be}$  states, such as clustering and collectivity. It uses a harmonic oscillator (HO) basis with frequency  $\hbar\Omega$  and a model space with an  $N_{\text{max}}$  cutoff, which is the maximum total HO excitation quanta above the lowest HO configuration for a given nucleus. These parameters are related to infrared (IR) and ultraviolet (UV) cutoffs [35], which can be understood as the effective size of the model space in which the nucleus resides, and its grid resolution, respectively. The calculations become independent of  $\hbar\Omega$  at  $N_{\text{max}} \rightarrow \infty$ , providing a parameter-free *ab initio* prediction. The SA-NCSM results exactly reproduce those of the NCSM [36,37] for the same nuclear interaction. However, by utilizing the emergent symplectic  $\text{Sp}(3, \mathbb{R})$  symmetry in nuclei [29], the SA-NCSM can expand the model space by a physically relevant subspace, which is only a fraction of the complete NCSM space, thereby including localized- $\alpha$  degrees of freedom within the interaction effective range [38].

We adopt various chiral potentials without renormalization in nuclear medium:  $\text{N}^3\text{LO-EM}$  [33],  $\text{NNLO}_{\text{opt}}$  [39], as well as  $\text{NNLO}_{\text{sat}}$  [40] with the three-nucleon (3N) forces, hierarchically smaller than their nucleon-nucleon (NN) forces, added as averages [30]. For comparison, we present results with the soft JISP16 phase-equivalent NN interaction [41]. We use  $\hbar\Omega = 15\text{--}25$  MeV for  $\text{N}^3\text{LO-EM}$ ,

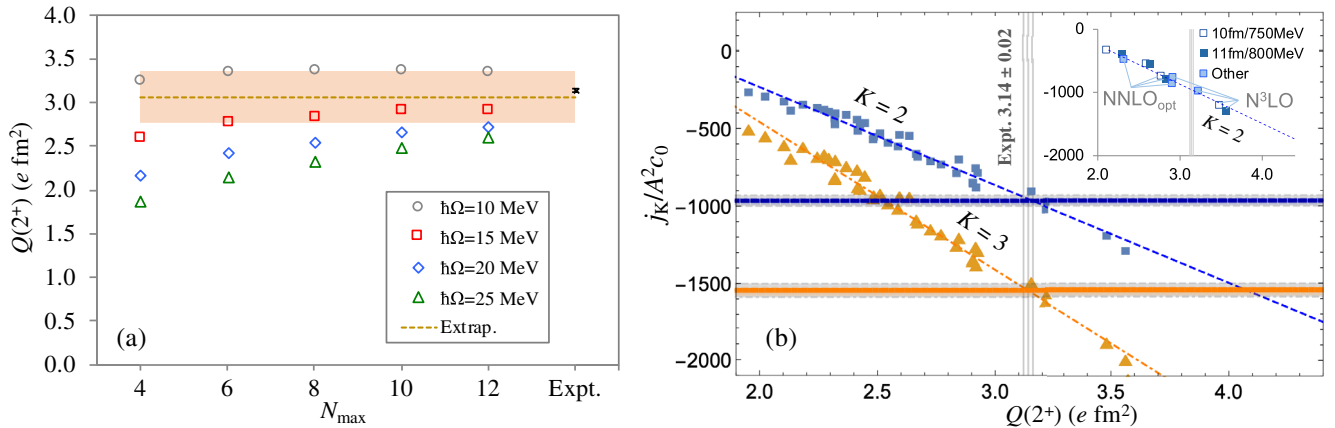


FIG. 2. (a) *Ab initio*  ${}^8\text{Li}$  g.s. quadrupole moment  $Q(2^+)$  compared with experiment [46] (denoted as “Expt.”). Calculations use the  $\text{NNLO}_{\text{opt}}$  NN for different model-space sizes and resolutions (open symbols), along with the infinite-size extrapolated value (dashed line) and the corresponding many-body uncertainty (shaded area). (b) Calculated  $j_2/A^2 c_0$  and  $j_3/A^2 c_0$  (squares and triangles, respectively) and their predicted values (upper and lower horizontal lines, respectively) for the  ${}^8\text{Li}$   $\beta$  decay to  $2^+_1$  in  ${}^8\text{Be}$  vs the calculated  ${}^8\text{Li}$   $Q(2^+)$ . The first (second) set of the uncertainties in Eq. (2) is shown as the line thickness (gray bands). Calculations use the  $\text{NNLO}_{\text{opt}}$ ,  $\text{NNLO}_{\text{sat}}$ , and  $\text{N}^3\text{LO}$  chiral potentials, and the JISP16 NN, in  $N_{\text{max}} = 6\text{--}12$  model spaces. Inset: subset of calculated  $j_2/A^2 c_0$  vs  $Q(2^+)$  for selected IR (in fm)/UV (in MeV) many-body cutoffs across all interactions, and for two interactions across several cutoffs.

$\text{NNLO}_{\text{opt}}$ , and JISP16, and  $\hbar\Omega = 16$  and 22 MeV for  $\text{NNLO}_{\text{sat}}$ , unless otherwise stated. The  $\text{NNLO}_{\text{opt}}$  is used without 3N forces, which have been shown to contribute minimally to the three- and four-nucleon binding energy [39]. Furthermore, the  $\text{NNLO}_{\text{opt}}$  NN potential has been found to reproduce various observables, including the  $^4\text{He}$  electric dipole polarizability [42]; the challenging analyzing power for elastic proton scattering on  $^4\text{He}$ ,  $^{12}\text{C}$ , and  $^{16}\text{O}$  [43]; along with  $B(E2)$  transition strengths for  $^{21}\text{Mg}$  and  $^{21}\text{F}$  [44] in the SA-NCSM without effective charges. For the purposes of this study, the quadrupole moment of the  $^8\text{Li}$  g.s.,  $Q(2_{\text{g.s.}}^+)$ , for which SA-NCSM calculations with the  $\text{NNLO}_{\text{opt}}$  NN are extrapolated to an infinite model-space size, is shown to reproduce the experimental value within the many-body model uncertainties [Fig. 2(a)]. The result is in close agreement with the extrapolated value of Ref. [45] that uses renormalized NN + 3N chiral potentials. The

model uncertainties are based on variations in the model-space size and resolution, and extrapolations use the Shanks method [29].

*Recoil-order corrections.*—The recoil-order form factors are generally neglected in  $\beta$ -decay theory since they are of the order of  $q/m_N$  or higher, where  $q$  is the momentum transfer (typically several MeV/ $c$ ) and  $m_N$  is the nucleon mass [14]. Thus, for most  $\beta$  decays, the recoil effects are typically less than a percent of the dominant Fermi and Gamow-Teller (GT) contributions (for an example, see Ref. [47]). However, for measurements of sufficiently high precision, these terms must be included in the analysis especially when the leading contributions are suppressed or the recoil-order terms are unusually large. These recoil-order form factors include the second forbidden axial vectors ( $j_2$  and  $j_3$ ), induced tensor ( $d$ ), and weak magnetism ( $b$ ), and along with the GT ( $c_0$ ), are given in the impulse approximation (IA) as

$$\begin{aligned}
 c_0(q^2) &= (-)^{(J'-J)} \frac{g_A(q^2)}{\sqrt{2J+1}} \langle J' || \sum_{i=1}^A \tau_i^\pm \sigma_i || J \rangle = (-)^{(J'-J)} \frac{g_A(q^2)}{\sqrt{2J+1}} M_{\text{GT}}, \\
 j_K(q^2) &= -(-)^{(J'-J)} \frac{2}{3} \frac{g_A(q^2)}{\sqrt{2J+1}} \frac{(Am_N c^2)^2}{(\hbar c)^2} \langle J' || \sum_{i=1}^A \tau_i^\pm [Q_i \times \sigma_i]^K || J \rangle, \quad \text{with } K = 2, 3, \\
 d(q^2) &= (-)^{(J'-J)} A \frac{g_A(q^2)}{\sqrt{2J+1}} \langle J' || \sum_{i=1}^A \tau_i^\pm \sqrt{2} [L_i \times \sigma_i]^1 || J \rangle, \\
 b(q^2) &= A \frac{(-)^{(J'-J)}}{\sqrt{2J+1}} \left[ g_M(q^2) \langle J' || \sum_{i=1}^A \tau_i^\pm \sigma_i || J \rangle + g_V(q^2) \langle J' || \sum_{i=1}^A \tau_i^\pm L_i || J \rangle \right], \quad (1)
 \end{aligned}$$

where  $g_V(0) = 1$ ,  $g_A(0) \approx 1.27$ , and  $g_M(0) \approx 4.70$  are the vector, axial, and weak magnetism coupling constants;  $A$  is the mass number; and  $J(J')$  is the total angular momentum of the initial (final) nucleus. The  $\tau_i/2$ ,  $\sigma_i/2$ ,  $Q_i = \sqrt{16\pi/5} r_i^2 Y_{2\mu}(\hat{r}_i)$ , and  $L_i$  are the isospin, intrinsic spin, quadrupole moment, and angular momentum operators, respectively, of the  $i$ th particle.  $M_{\text{GT}}$  is the conventional GT matrix element. The matrix elements in Eq. (1) are computed translationally invariant in the SA-NCSM. These recoil-order form factors, usually reported as the ratios  $j_{2,3}/A^2 c_0$ ,  $d/Ac_0$ , and  $b/Ac_0$ , enter into the expression of the  $\beta$ -decay rate for nuclei undergoing delayed  $\alpha$ -particle emission [8,14,19,48].

Remarkably, we identify a strong correlation between  $j_{2,3}/A^2 c_0$  and the  $^8\text{Li}$  g.s. quadrupole moment based on calculations across several interactions,  $N_{\text{max}}$  and  $\hbar\Omega$  parameters [Fig. 2(b), using  $N_{\text{max}} = 6\text{--}12$  for  $\text{NNLO}_{\text{opt}}$ ,  $6\text{--}10$  for N3LO-EM and JISP16, and  $6\text{--}8$  for  $\text{NNLO}_{\text{sat}}$ ]. As can be seen in the Fig. 2(b) inset, the linear dependence is observed regardless of any errors that may arise from the

many-body truncation and from the higher-order effects (e.g., Refs. [49,50]) associated with various interactions. An identical spread is found for  $j_3/A^2 c_0$  due to the strong correlation between  $j_2$  and  $j_3$  (see Supplemental Material [51]). A linear regression along with the combination of the correlation to  $Q(2_{\text{g.s.}}^+)$  and its experimental value of  $3.14(2) e \text{ fm}^2$  [46] lead to reduced uncertainties on our predictions:

$$\frac{j_2}{A^2 c_0} = -966 \pm 13 \pm 33, \quad \frac{j_3}{A^2 c_0} = -1546 \pm 19 \pm 40. \quad (2)$$

Here, the first set of uncertainties uses the quadrupole moment experimental uncertainties given the linear regression slope, and the second set arises from the regression uncertainty using Student's  $t$  distribution and a 99% confidence level. This correlation is important, as we can reduce the problem of calculating a matrix element that depends on cluster physics in  $^8\text{Be}$  to a bound state observable in  $^8\text{Li}$ .

TABLE I. The recoil-order terms from SA-NCSM. Results for the  $2_1^+$   $j_{2,3}/A^2c_0$  and  $d/Ac_0$  are based on the correlation to  $Q(2_{\text{g.s.}}^+)$ ; all other calculations use  $\text{NNLO}_{\text{opt}}$  and have error bars from variations in  $\hbar\Omega$  by 5 MeV and in model-space sizes up to  $N_{\text{max}} = 16$  (12) for  $j_{2,3}/A^2c_0$  ( $d/Ac_0$  and  $b/Ac_0$ ).

	$j_2/A^2c_0$	$j_3/A^2c_0$	$d/Ac_0$	$b/Ac_0$
$2_1^+$	$-966 \pm 36$	$-1546 \pm 44$	$10.0 \pm 1.0$	$6.0 \pm 0.4$
$2_2^+$ (new)	$-10 \pm 10$	$-80 \pm 30$	$-0.5 \pm 0.5$	$3.7 \pm 0.4$
$2_3^+$ (doublet 1)	$12 \pm 5$	$-60 \pm 15$	$0.3 \pm 0.2$	$3.8 \pm 0.2$
$2_4^+$ (doublet 2)	$11 \pm 3$	$-65 \pm 11$	$0.2 \pm 0.2$	$3.8 \pm 0.2$

Most significantly, with the values in Eq. (2), the uncertainty from the recoil-order corrections on the tensor current contribution to the weak interaction presented in Ref. [48] is reduced by over 50% [19]. The recoil-order terms, including the  $b$  and  $d$  terms, for the lowest four SA-NCSM  $2^+$  states, are summarized in Table I. The  $d/Ac_0$  prediction for  $2_1^+$  is based on a correlation similar to the one for  $j_{2,3}/A^2c_0$  (see Supplemental Material [51]). These predictions can be used in future experiments to constrain beyond the standard model tensor currents, while these  $b$  weak magnetism predictions are of interest to experiments that test the CVC hypothesis, and  $d$  is of importance to determining the existence of second-class currents [12].

*New final state for  $\beta$  decays to  ${}^8\text{Be}$ .*—The experimentally deduced values presented in Ref. [16],  $j_2/A^2c_0 = -490 \pm 70$ ,  $j_3/A^2c_0 = -980 \pm 280$ ,  $d/Ac_0 = 5.5 \pm 1.7$ , and  $b/Ac_0 = 7.5 \pm 0.2$ , are comparable but different from our predicted values. These experimental results were obtained through a global fit to  $\beta$ -spin alignment [16]

and  $\beta - \alpha$  angular correlation data [20] from  ${}^8\text{Li}$  and  ${}^8\text{B}$   $\beta$  decays. Because of the small size of higher-order effects and relatively large statistical uncertainties, the  $j_{2,3}/A^2c_0$  and  $d/Ac_0$  were assumed in Ref. [16] to be independent of the  ${}^8\text{Be}$  excitation energy. Thus, the results were averaged over the entire  $\beta$ -decay spectrum. In contrast, the SA-NCSM wave functions are for individual states; hence, the predictions in Eq. (2) are for the lowest  $2^+$  state only, which is the dominant transition for the  ${}^8\text{Li}$   $\beta$  decay. The SA-NCSM reveals large differences between the recoil-order terms to the lowest  $2_1^+$  and higher-lying states, the most notable being for the  $j_K/A^2c_0$  terms where the values differ by almost 2 orders of magnitude (see Table I). Hence, the angular-correlation experiment in Ref. [19] minimizes the sensitivity to the higher-lying states by restricting their analysis to decays centered on the broad  $2_1^+$  state.

Importantly, the SA-NCSM indicates the existence of another  $2^+$  state below 16 MeV—accessible to the  ${}^8\text{Li}$  or  ${}^8\text{B}$   $\beta$  decays through allowed transitions—and a corresponding lower  $0^+$  state that largely overlaps with the  $\alpha + \alpha$  system (Fig. 3, see also Supplemental Material [51]). In the SA-NCSM, these states quickly decrease in energy as the model space increases [Fig. 3(a)] regardless of the realistic interaction used, similar to the Hoyle-state rotational band in  ${}^{12}\text{C}$  [56]. The extrapolations are performed using the three-parameter exponential formula from Ref. [57]. Notably,  $0_3^+$  converges to  $20.1 \pm 1.5$  MeV and has a structure similar to the doublet  $2^+$  states and isospin  $T = 1$ . This state is not seen in the currently available experimental spectrum, and it is likely to be the isobaric analog of the low-lying  $0^+$  state in  ${}^8\text{Li}$  predicted by recent *ab initio* calculations [45,58].

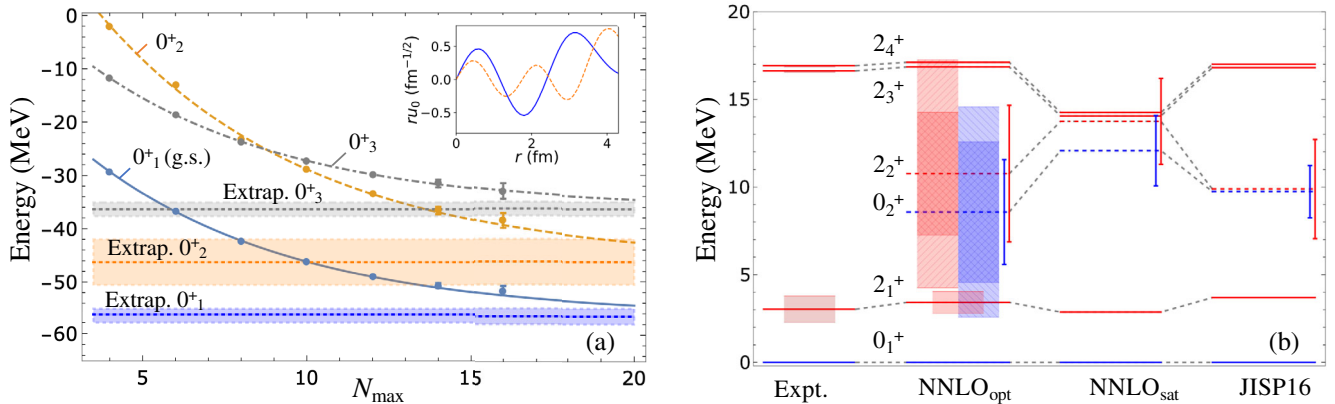


FIG. 3. (a) Calculated  ${}^8\text{Be}$  low-lying  $0^+$  state energies illustrated for the  $\text{NNLO}_{\text{opt}}$  chiral potential ( $\hbar\Omega = 15$  MeV) vs the model-space size, together with the extrapolation values (dotted lines) and uncertainties (bands). Extrapolations use complete model spaces up to  $N_{\text{max}} = 12$  and do not include the  $N_{\text{max}} = 14$  and 16 SA selected model spaces shown with uncertainties determined by the selection. The measured  $0_{\text{g.s.}}^+$  energy is  $-56.5$  MeV [59]. Inset:  $\alpha + \alpha$  wave for  $0_{\text{g.s.}}^+$  (blue solid) and  $0_2^+$  (orange dashed). (b) *Ab initio* low-lying states from extrapolations for  ${}^8\text{Be}$ , compared with experiment (Expt.). The extrapolation uncertainties (error bars) for the  $0_2^+$  and  $2_2^+$  states (dashed levels) are based on variations in the model-space size and selection. For  $\text{NNLO}_{\text{opt}}$ ,  $\alpha$  width estimates (shaded areas) for the lowest two  $0^+$  and  $2^+$  states are shown with uncertainties (lighter shades) determined from the energy extrapolation uncertainties; the small  $0_{\text{g.s.}}^+$  width (not shown) is estimated to be 5.7 eV, compared with 5.57 eV [60].

The calculated low-lying states in  ${}^8\text{Be}$  are in good agreement with experiment [Fig. 3(b)]. The NNLO<sub>sat</sub> results include the average 3N contribution determined for a given isospin (for  ${}^8\text{Be}$ , the contribution to the binding energy in  $N_{\text{max}} = 12$  is 1.51 MeV, resulting in a total extrapolated binding energy of 56.8 MeV). The extrapolations determine the energies of  $0_2^+$  and  $2_2^+$  between 5 and 15 MeV above the g.s., corroborating earlier estimates [21,22,24].

For NNLO<sub>opt</sub> NN and the case of the fastest energy convergence of the  $0_2^+$  and  $2_2^+$  states ( $\hbar\Omega = 15$  MeV), we estimate  $\alpha$  widths [Fig. 3(b)] by projecting the  $N_{\text{max}} = 16$  SA-NCSM wave functions onto  $\alpha + \alpha$  cluster states and considering the exact continuum Coulomb wave functions outside of the interaction effective range, following the procedure of Ref. [38]. For this, the  ${}^8\text{Be}$  and  ${}^4\text{He}$  states are expressed in the  $\text{Sp}(3, \mathbb{R})$  basis, associated with intrinsic shapes [29]. For  ${}^8\text{Be}$ , we consider three dominant prolate shapes with contributions of 75%, 4%, and 3% to  $0_{\text{g.s.}}^+$  (totaling 82%), and 46%, 15%, and 11% to  $0_2^+$  (totaling 72%), and similarly for the  $2^+$  states (see Supplemental Material [51]). These shapes extend to 18 HO shells and start at the most deformed configurations among those in the valence shell:  $2\hbar\Omega$  and  $4\hbar\Omega$  excitations. Except for the  $0_{\text{g.s.}}^+$  width that uses the experimental threshold of  $-92$  keV relative to the  ${}^8\text{Be}$  g.s., all the widths use the  $\alpha + \alpha$  threshold estimated at  $-104$  keV from the SA-NCSM extrapolations of the  ${}^4\text{He}$  and  ${}^8\text{Be}$  binding energies with NNLO<sub>opt</sub>. These widths are in good agreement with experimentally deduced values [60] and earlier theoretical studies [61–63].

Intruder  $0^+$  and  $2^+$  states in the low-lying spectrum of  ${}^8\text{Be}$  were proposed in the late 1960s by Barker from concurrent  $R$ -matrix fits to scattering, reaction, and decay data associated with the  ${}^8\text{Be}$  nucleus [21,22]. The inclusion of an intruder  $2^+$  state below 16 MeV in the  $R$ -matrix fits of  $\beta$  decays in Ref. [64] results in a decrease of the extracted  $M_{\text{GT}}$  for a decay to  $2_1^+$  by almost 1.5 times, which yields a closer agreement with the SA-NCSM  $M_{\text{GT}}$  (see Table II; the calculated  $M_{\text{GT}}$  are not used in the experimental analysis of Ref. [19]). Note that, depending on the interaction, two-body axial currents may significantly affect  $M_{\text{GT}}$  [65]; however, here we are interested only in the IA part. Because of the large uncertainty on the  $2_2^+$  state in the calculations, we provide only the lower limits on the  $\log(ft)$  based on the convergence pattern. The energies from Barker’s  $R$ -matrix fits for the intruder  $0^+$  and  $2^+$  states are  $\sim 6$  MeV and 9 MeV, respectively, with  $\alpha$  widths  $> 7$  MeV. These excitation energies agree with the SA-NCSM extrapolated results given the error bars [Fig. 3(b)], as well as with the predicted widths. The strong excitation-energy dependence of the recoil-order terms due to the presence of  $2_2^+$  has a small effect on the weak tensor current constraints in the low excitation-energy range (see systematic

TABLE II. *Ab initio*  $M_{\text{GT}}$ ,  $c_0$ , and  $\log(ft)$  in IA, compared with the experimentally deduced values (Expt.). Reference [64] includes evaluations both with an intruder  $2^+$  state (denoted by \*) around 8 MeV similar to Ref. [23], and without it.

	$2_1^+$		$2_2^+$	
	$ M_{\text{GT}} $	$ c_0 $	$\log(ft)$	$\log(ft)$
NNLO <sub>opt</sub>	0.16(1)	0.09(1)	5.90	$> 5.06$
NNLO <sub>sat</sub>	0.21(3)	0.12(2)	5.64	$> 5.05$
JISP16	0.23(4)	0.13(2)	5.54	$> 4.28$
Expt., Ref. [23]	0.190	0.108	5.72	5.27
Expt., Ref. [64]*	0.204	0.116	5.66	5.2
Expt., Ref. [64]	0.284	0.163	5.37	N/A

uncertainty in Table I in Ref. [19]), but is imperative to consider in analyses over the entire  $\beta$ -decay spectrum.

*Summary.*—The *ab initio* SA-NCSM has determined the size of the recoil-order form factors in the  $\beta$  decay of  ${}^8\text{Li}$ . It has shown that states of the  $\alpha + \alpha$  system not included in the evaluated  ${}^8\text{Be}$  energy spectrum have an important effect on all  $j_{2,3}/A^2c_0$ ,  $b/Ac_0$ , and  $d/Ac_0$  terms, and can explain the  $M_{\text{GT}}$  discrepancy in the  $A = 8$  systems. The outcomes reduce—by over 50%—the uncertainty on these recoil-order corrections, and help improve the sensitivity of high-precision  $\beta$ -decay experiments that probe the  $V - A$  structure of the weak interaction [19]. Furthermore, our predicted  $b/Ac_0$  and  $d/Ac_0$  values are important for other investigations of the standard model symmetries, such as the CVC hypothesis and the existence of second-class currents.

We thank Scott Marley and Konstantinos Kravvaris for useful discussions. This work was supported in part by the U.S. National Science Foundation (PHY-1913728), SURA, Czech Science Foundation (22-14497S), and the Czech Ministry of Education, Youth and Sports under Grant No. CZ.02.1.01/0.0/0.0/16\_019/0000765. It benefited from high performance computational resources provided by LSU ([www.hpc.lsu.edu](http://www.hpc.lsu.edu)), the National Energy Research Scientific Computing Center (NERSC), a U.S. Department of Energy Office of Science User Facility operated under Contract No. DE-AC02-05CH11231, as well as the Frontera computing project at the Texas Advanced Computing Center, made possible by National Science Foundation Award No. OAC-1818253. L. V. was supported by a National Science Foundation Graduate Research Fellowship under Grant No. DGE-1746045. This work was performed under the auspices of the U.S. Department of Energy by Lawrence Livermore National Laboratory under Contract No. DE-AC52-07NA27344.

- [1] R. P. Feynman and M. Gell-Mann, *Phys. Rev.* **109**, 193 (1958).  
 [2] E. C. Sudarshan and R. Marshak, *Phys. Rev.* **109**, 1860 (1958).

- [3] C. S. Wu, E. Ambler, R. W. Hayward, D. D. Hoppes, and R. P. Hudson, *Phys. Rev.* **105**, 1413 (1957).
- [4] W. B. Herrmannsfeldt, D. R. Maxson, P. Stählerin, and J. S. Allen, *Phys. Rev.* **107**, 641 (1957).
- [5] C. Johnson, F. Pleasonton, and T. Carlson, *Phys. Rev.* **132**, 1149 (1963).
- [6] X. Fléchar, P. Velten, E. Liénard, A. Méry, D. Rodríguez, G. Ban, D. Durand, F. Mauger, O. Naviliat-Cuncic, and J. Thomas, *J. Phys. G* **38**, 055101 (2011).
- [7] G. Li *et al.*, *Phys. Rev. Lett.* **110**, 092502 (2013).
- [8] M. G. Sternberg, R. Segel, N. D. Scielzo, G. Savard, J. A. Clark, P. F. Bertone, F. Buchinger, M. Burkey, S. Caldwell, A. Chaudhuri *et al.*, *Phys. Rev. Lett.* **115**, 182501 (2015).
- [9] N. Severijns, M. Beck, and O. Naviliat-Cuncic, *Rev. Mod. Phys.* **78**, 991 (2006).
- [10] F. Wauters, A. García, and R. Hong, *Phys. Rev. C* **89**, 025501 (2014).
- [11] L. Grenacs, *Annu. Rev. Nucl. Part. Sci.* **35**, 455 (1985).
- [12] L. De Braekeleer, E. G. Adelberger, J. H. Gundlach, M. Kaplan, D. Markoff, A. M. Nathan, W. Schieff, K. A. Snover, D. W. Storm, K. B. Swartz, D. Wright, and B. A. Brown, *Phys. Rev. C* **51**, 2778 (1995).
- [13] T. Sumikama, K. Matsuta, T. Nagatomo, M. Ogura, T. Iwakoshi, Y. Nakashima, H. Fujiwara, M. Fukuda, M. Mihara, K. Minamisono *et al.*, *Phys. Lett. B* **664**, 235 (2008).
- [14] B. R. Holstein, *Rev. Mod. Phys.* **46**, 789 (1974).
- [15] R. E. Tribble and G. T. Garvey, *Phys. Rev. C* **12**, 967 (1975).
- [16] T. Sumikama, K. Matsuta, T. Nagatomo, M. Ogura, T. Iwakoshi, Y. Nakashima, H. Fujiwara, M. Fukuda, M. Mihara, K. Minamisono, T. Yamaguchi, and T. Minamisono, *Phys. Rev. C* **83**, 065501 (2011).
- [17] C. A. Barnes, W. A. Fowler, H. B. Greenstein, C. C. Lauritsen, and M. E. Nordberg, *Phys. Rev. Lett.* **1**, 328 (1958).
- [18] N. Scielzo, G. Li, M. Sternberg, G. Savard, P. Bertone, F. Buchinger, S. Caldwell, J. Clark, J. Crawford, C. Deibel *et al.*, *Nucl. Instrum. Methods Phys. Res., Sect. A* **681**, 94 (2012).
- [19] M. Burkey, G. Savard, A. Gallant, N. Scielzo, J. Clark, T. Hirsh, L. Varriano, G. Sargsyan, K. Launey, M. Brodeur, D. Burdette *et al.*, preceding Letter, *Phys. Rev. Lett.* **128**, 202502 (2022).
- [20] R. D. McKeown, G. T. Garvey, and C. A. Gagliardi, *Phys. Rev. C* **22**, 738 (1980).
- [21] F. Barker, H. Hay, and P. Treacy, *Aust. J. Phys.* **21**, 239 (1968).
- [22] F. Barker, *Aust. J. Phys.* **22**, 293 (1969).
- [23] F. Barker, *Aust. J. Phys.* **42**, 25 (1989).
- [24] E. Caurier, P. Navrátil, W. E. Ormand, and J. P. Vary, *Phys. Rev. C* **64**, 051301(R) (2001).
- [25] P. Maris, *J. Phys. Conf. Ser.* **445**, 012035 (2013).
- [26] D. Rodkin and Y. M. Tchuvil'sky, *Chin. Phys. C* **44**, 124105 (2020).
- [27] M. Munch, O. Sølund Kirsebom, J. A. Swartz, K. Riisager, and H. O. U. Fynbo, *Phys. Lett. B* **782**, 779 (2018).
- [28] K. D. Launey, T. Dytrych, and J. P. Draayer, *Prog. Part. Nucl. Phys.* **89**, 101 (2016).
- [29] T. Dytrych, K. D. Launey, J. P. Draayer, D. J. Rowe, J. L. Wood, G. Rosensteel, C. Bahri, D. Langr, and R. B. Baker, *Phys. Rev. Lett.* **124**, 042501 (2020).
- [30] K. D. Launey, A. Mercenne, and T. Dytrych, *Annu. Rev. Nucl. Part. Sci.* **71**, 253 (2021).
- [31] P. F. Bedaque and U. van Kolck, *Annu. Rev. Nucl. Part. Sci.* **52**, 339 (2002).
- [32] E. Epelbaum, A. Nogga, W. Glöckle, H. Kamada, Ulf-G. Meißner, and H. Witała, *Phys. Rev. C* **66**, 064001 (2002).
- [33] D. R. Entem and R. Machleidt, *Phys. Rev. C* **68**, 041001(R) (2003).
- [34] E. Epelbaum, *Prog. Part. Nucl. Phys.* **57**, 654 (2006).
- [35] K. A. Wendt, C. Forssén, T. Papenbrock, and D. Sääf, *Phys. Rev. C* **91**, 061301(R) (2015).
- [36] P. Navrátil, J. P. Vary, and B. R. Barrett, *Phys. Rev. Lett.* **84**, 5728 (2000).
- [37] P. Navrátil, J. P. Vary, and B. R. Barrett, *Phys. Rev. C* **62**, 054311 (2000).
- [38] A. C. Dreyfuss, K. D. Launey, J. E. Escher, G. H. Sargsyan, R. B. Baker, T. Dytrych, and J. P. Draayer, *Phys. Rev. C* **102**, 044608 (2020).
- [39] A. Ekström, G. Baardsen, C. Forssén, G. Hagen, M. Hjorth-Jensen, G. R. Jansen, R. Machleidt, W. Nazarewicz, T. Papenbrock, J. Sarich, and S. M. Wild, *Phys. Rev. Lett.* **110**, 192502 (2013).
- [40] A. Ekström, G. R. Jansen, K. A. Wendt, G. Hagen, T. Papenbrock, B. D. Carlsson, C. Forssén, M. Hjorth-Jensen, P. Navrátil, and W. Nazarewicz, *Phys. Rev. C* **91**, 051301(R) (2015).
- [41] A. Shirokov, V. Kulikov, P. Maris, A. Mazur, E. Mazur, and J. Vary, *EPJ Web Conf.* **3**, 05015 (2010).
- [42] R. B. Baker, K. D. Launey, S. Bacca, N. N. Dinur, and T. Dytrych, *Phys. Rev. C* **102**, 014320 (2020).
- [43] M. Burrows, C. Elster, S. P. Weppner, K. D. Launey, P. Maris, A. Nogga, and G. Popa, *Phys. Rev. C* **99**, 044603 (2019).
- [44] P. Ruotsalainen *et al.*, *Phys. Rev. C* **99**, 051301(R) (2019).
- [45] C. McCracken, P. Navrátil, A. McCoy, S. Quaglioni, and G. Hupin, *Phys. Rev. C* **103**, 035801 (2021).
- [46] D. Borremans, D. L. Balabanski, K. Blaum, W. Geithner, S. Gheysen, P. Himpe, M. Kowalska, J. Lassen, P. Lievens, S. Mallion, R. Neugart, G. Neyens, N. Vermeulen, and D. Yordanov, *Phys. Rev. C* **72**, 044309 (2005).
- [47] A. Glick-Magid, C. Forssén, D. Gazda, D. Gazit, P. Gysbers, and P. Navrátil, [arXiv:2107.10212](https://arxiv.org/abs/2107.10212).
- [48] M. T. Burkey, Searching for tensor currents in the weak interaction using lithium-8  $\beta$  decay, Ph.D. thesis, Chicago University, 2019.
- [49] A. A. Filin, D. Möller, V. Baru, E. Epelbaum, H. Krebs, and P. Reinert, *Phys. Rev. C* **103**, 024313 (2021).
- [50] P. Maris, E. Epelbaum, R. J. Furnstahl, J. Golak, K. Hebeler, T. Hüther, H. Kamada, H. Krebs, Ulf-G. Meißner, J. A. Melendez, A. Nogga, P. Reinert, R. Roth, R. Skibiński, V. Soloviev, K. Topolnicki, J. P. Vary, Yu. Volkotrub, H. Witała, and T. Wolfgruber (LENPIC Collaboration), *Phys. Rev. C* **103**, 054001 (2021).
- [51] See Supplemental Material at <http://link.aps.org/supplemental/10.1103/PhysRevLett.128.202503>, which includes Refs. [52–55], for additional correlation plots, intercluster wavefunctions used in calculations of widths,

- as well as the decomposition of the ground and intruder states in the SA basis.
- [52] J. Suhonen, *From Nucleons to Nucleus: Concepts of Microscopic Nuclear Theory* (Springer Science & Business Media, New York, 2007).
- [53] P. Navrátil, *Phys. Rev. C* **70**, 054324 (2004).
- [54] O. Castaños, J. P. Draayer, and Y. Leschber, *Z. Phys. A* **329**, 33 (1988).
- [55] M. T. Mustonen, C. N. Gilbreth, Y. Alhassid, and G. F. Bertsch, *Phys. Rev. C* **98**, 034317 (2018).
- [56] A. C. Dreyfuss, K. D. Launey, T. Dytrych, J. P. Draayer, and C. Bahri, *Phys. Lett. B* **727**, 511 (2013).
- [57] P. Maris, J. P. Vary, and A. M. Shirokov, *Phys. Rev. C* **79**, 014308 (2009).
- [58] P. Navrátil, R. Roth, and S. Quaglioni, *Phys. Rev. C* **82**, 034609 (2010).
- [59] W. Huang, M. Wang, F. Kondev, G. Audi, and S. Naimi, *Chin. Phys. C* **45**, 030002 (2021).
- [60] D. Tilley, J. Kelley, J. Godwin, D. Millener, J. Purcell, C. Sheu, and H. Weller, *Nucl. Phys. A* **745**, 155 (2004).
- [61] K. Kravvaris and A. Volya, *Phys. Rev. Lett.* **119**, 062501 (2017).
- [62] K. Kravvaris, S. Quaglioni, G. Hupin, and P. Navratil, [arXiv:2012.00228](https://arxiv.org/abs/2012.00228).
- [63] S. Elhatisari, D. Lee, G. Rupak, E. Epelbaum, H. Krebs, T. A. Lähde, T. Luu, and U.-G. Meißner, *Nature (London)* **528**, 111 (2015).
- [64] E. K. Warburton, *Phys. Rev. C* **33**, 303 (1986).
- [65] G. B. King, L. Andreoli, S. Pastore, M. Piarulli, R. Schiavilla, R. B. Wiringa, J. Carlson, and S. Gandolfi, *Phys. Rev. C* **102**, 025501 (2020).